Asian Journal of Chemistry; Vol. 37, No. 8 (2025), 1898-1902

ASIAN JOURNAL OF CHEMISTRY

https://doi.org/10.14233/ajchem.2025.34005

Physicochemical Studies of Ni/Al Layered Double Hydroxide at Ambient Temperature

SITI NURUL 'AFINI MOHD JOHARI[1], SITI KHATIJAH DERAMAN[2,*], HUSSEIN HANIBAH[2] and NAZRIZAWATI AHMAD TAJUDDIN[1]

[1]School of Chemistry and Environment, Faculty of Applied Sciences, Universiti Teknologi MARA (UiTM), 40450 Shah Alam, Selangor, Malaysia
[2]Centre of Foundation Studies, Universiti Teknologi MARA, Cawangan Selangor, Kampus Dengkil 43800 Dengkil, Selangor, Malaysia

*Corresponding author: E-mail: drsitikhatijah@uitm.edu.my

Received: 7 May 2025; *Accepted*: 1 July 2025; *Published online*: 31 July 2025; AJC-22068

The Ni/Al layered double hydroxide (Ni/Al LDH) was synthesized *via* alkali free co-precipitation method with ratio of 4:1. The product of co-precipitation was undergone aging process for 24 h. Then, it was placed in oven at 100 ºC overnight and finally was calcined at 450 ºC for 13 h. The correlation of crystallinity; morphology and particle size of Ni/Al LDH before and after calcination were examined and compared. Thermogravimetric analysis (TGA) was used to evaluate the interlayer anion and carbonate content of Ni/Al LDH. Powder X-ray diffraction (PXRD) was used to study the textural and structural characteristics of the samples. Particle size, morphology and particle properties were characterized by Brunauer-Emmett-Teller (BET) and field emission scanning electron (FESEM). The bonding and structural of Ni/Al LDH was studied by Fourier transform infrared (FTIR).

Keywords: Layered double hydroxide, Hydrotalcites, Nanocomposite, Co-precipitation.

INTRODUCTION

Layered double hydroxides (LDHs), commonly referred to as hydrotalcites, are a type of anionic clay characterized by significant absorption capacity. In general, LDH consists of positively charged metal hydroxide sheets with anions located between the layers to compensate the positive layer charges that similar to brucite [1]. These layers are balanced by anions in between them and there are also water molecules present in the spaces between the layers [2]. The composition of LDH is generally represented by the following equation:

$$[M^{2+}_{1-x}M^{3+}_{x}(OH)_2(A^{n-})_{x/n}]\cdot mH_2O$$

where M^{2+} and M^{3+} represent bivalent and trivalent metal cations, respectively and A^{n-} is the interlayer anion. With regard to its malleable structure, hydrotalcite has highly customizable features that find use in a wide variety of applications. Several literature reported the wide applications of LDH as catalyst precursors, catalyst supports, adsorbents and ion exchangers in different research directions such as gas removing, selective hydrogenation, electrocatalysis oxidation, *etc*. [3].

LDHs are appealing adsorbents due to their economical nature, stratified composition, extensive surface area and notable anion exchange capability. LDHs may uptake the anion *via* three mechanisms: interlayer ion exchange, surface adsorption and the memory effect. LDHs may undergo calcination at a certain temperature to transform into layered double oxides (LDOs) [4]. Another well recognized method for LDH synthesis is the calcination recovery, which relies on the phenomenon known as the "memory effect." During the calcination process, the interlayer anion is removed. This transformation converts the LDH into a layered double oxide (LDO), causing the layered structure to disintegrate into a cubic phase. Upon addition of the LDO to an aqueous solution, the layered structure is reconstructed, including a distinct intercalated anion, resulting in the formation of a new LDH. Dehydration, dihydroxylation, anion breakdown and oxide segregation are all part of the calcination treatment process. These breakdown processes amplify the surface imperfections of LDHs. The memory effect allows LDOs to easily recreate their original layered structure by intercalating anions (CO_3^{2-} and OH^-) into their structure. LDOs have better adsorption capacity due to their abundance of metallic oxide and memory effect, which can absorb anions into their structure [4].

In this work, nickel/aluminum layered double hydroxide (Ni/Al LDH) will be synthesized using free-alkali co-precipitation method. This method approach is the predominant technique

for synthesizing LDHs. It involves combining a solution containing mixed alkali soda with a solution containing mixed salts. The resulting mixture is then allowed to mature at a certain temperature [3].

EXPERIMENTAL

Nickel nitrate hexahydrate ($Ni(NO_3)_2{\cdot}6H_2O$) (> 97% pure), ammonium carbonate ($(NH_4)_2CO_3$) (> 98% pure), aluminum nitrate nonahydrate ($Al(NO_3)_3{\cdot}9H_2O$) (> 98.5% pure) and ammonium solution (NH_4OH) were procured from Systerm Chem Pur, Malaysia. All the mentioned product been used without any further purification in this research.

Preparation of Ni/Al LDH: Alkali free co-precipitation method was used to synthesize LDHs with molar ratio 4:1 Ni/Al [5]. The synthesis was prepared by mixing an aqueous solution of metallic cations (solution A) with a highly basic carbonate solution (solution B) simultaneously dropwise under vigorous stirring at pH 7.5. Ammonium hydroxide solution was added drop by drop in order to maintain the pH. Solution A was prepared by mixing 1 M $Ni(NO_3)_2{\cdot}6H_2O$ with 1 M $Al(NO_3)_3{\cdot}9H_2O$ according to 4:1 molar ratio to make up 100 mL solution. Solution B was 2 M $(NH_4)_2CO_3$ in 100 mL distilled water. A constant pH 9.5 was maintained throughout by this room temperature synthesis by the dropwise addition of aqueous NH_4OH. The product of co-precipitation was brought to reflux for 24 h for aging process at 65 ºC. Then, the solution was filtered and washed with distilled water until pH of the filtrate reach 7. Then, the precursor was oven-annealed at 100 ºC for 24 h to obtain green coloured Ni/Al LDH.

Activation of Ni/Al LDH precursors by calcination: The Ni/Al LDHs precursor was calcined at 450 ºC for 13 h using muffle furnace to remove water molecule and carbonate compound. All samples must be placed into the vacuum desiccator to prevent the catalyst from absorbing moisture. This is because Ni/Al LDH is hygroscopic in nature.

Characterization: Thermogravimetric analysis (TGA) of the as-synthesized Ni/Al LDH was carried out in the Setaram Setsys Evolution 18 (TG-DSC/DTA). It was used to evaluate the interlayer water and carbonate content, at a heating rate 800 ºC at 10 ºC min^{-1} under nitrogen condition. Powder X-ray diffraction (PXRD) performed by PANalytical X'pert PRO model was operated at 40 kV and 40 mA using Cu*K*α. The measurements were made with diffraction angle 2θ from 8 to 90º at speed 1.2º min^{-1}. For LDH, FTIR were performed using Perkin-Elmer model Spectrum One spectrometer in the range 4500-400 cm^{-1} using KBr pellet method. The surface area (SA) and pore size distribution measurements were obtained with Quantachrome Autosorb iQ2 instrument. N_2 gas was used as the adsorbate at 77 K. The Brunauer-Emmett-Teller (BET) method was used to measure the surface are by a multipoint method and the Barret-Joyner-Halenda (BJH) desorption method was used to calculate the pore size distribution. Sample were degassed at 120 ºC for 12 h to remove any adsorbed species before analysis. The surface morphologies of the synthesized materials (Ni/Al LDH and polymer electrolyte) were studied using field emission scanning electron (FESEM) on a Jeol JSM - 7600F instrument with a Schottky emitter at an accelerating voltage of 2.0 kV with a beam current of 1.0 mA. The samples were ultrasonically dispersed in ethanol and deposited Au-coated silicon chips prior to analysis.

RESULTS AND DISCUSSION

Thermal studies: Fig. 1 shows the Ni/Al LDHs thermograms, which show that the Ni/Al split at high temperatures in two steps. The first region of weight loss, at temperatures lower than 123 ºC, is due to the removal of the physiosorbed and interlayer water (H_2O) molecules (dehydration), which does not change the layered structure of the Ni/Al. For the second region (dihydroxylation), the release of the hydroxyl group (OH^-) from the brucite layers and NO_3 from the interlayer anions is thought to cause weight loss at temper-atures between 123 ºC and 252 ºC. The DTG curves also show that as-synthesized LDH breaks down completely at 252 ºC. Above 252 ºC, there is no weight loss due to decarbonation, CO_3^-, which means that there is no change in phase after 252 ºC, so the calcination temperature for the calcined Ni/Al adsorbent is set at 450 ºC. This proposed method was considered acceptable and comparable with the other studies [6]. Meanwhile, starting from 200 to 450 ºC, the dihydroxylation of LDH layers and decarbonation of carbonate anions present in its interlayer gallery layers was formed. Table-1 shows the decomposition temperature of LDH measured by TGA instrument.

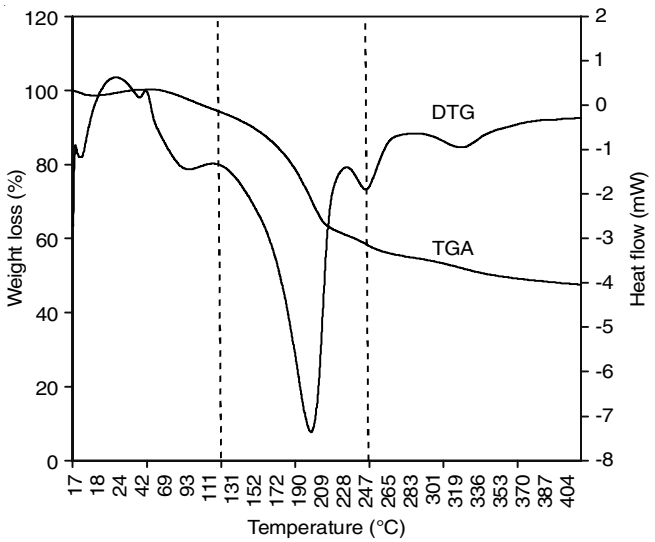

Fig. 1. TGA/DTG thermograms of raw Ni/Al LDH

TABLE-1
THE DECOMPOSITION TEMPERATURE OF LDH MEASURED BY TGA INSTRUMENT

Materials	Decomposition (ºC)	Weight loss stages	First weight loss (ºC) (dehydration)	Second weight loss (ºC) (dihydroxylation)	Third weight loss (ºC) (decarboxylation/ decarbonation)
Raw Ni/Al LDH	450	Three	123	252	>252

Powder-XRD studies: The crystalline structure of raw and calcined Ni/Al LDH precursors was investigated by using PXRD. The patterns of synthesized Ni/Al LDHs (raw and calcined are shown in Fig. 2. The diffraction patterns for the as-synthesized LDH samples display the characteristics diffraction peaks around 11º and 23º, which can be indexed as a hexagonal lattice with rhombohedral symmetry of crystalline hydrotalcite-like LDHs. It consists of peaks at 2θ 11.7º (003), 23.5º (006), 35.1º (012), 39.7º (015), 47.3º (018), 61.2º (110), 62.5º (113) (JCPDS card No. 15-0087), which confirmed the successfully preparation of hydrotalcite structure of Ni/Al LDH. This result agrees well with the reported literature [7,8]. Table-2 shows the textural properties of *d*-spacing and lattice parameters of the Ni/Al LDH and CNi/Al LDH.

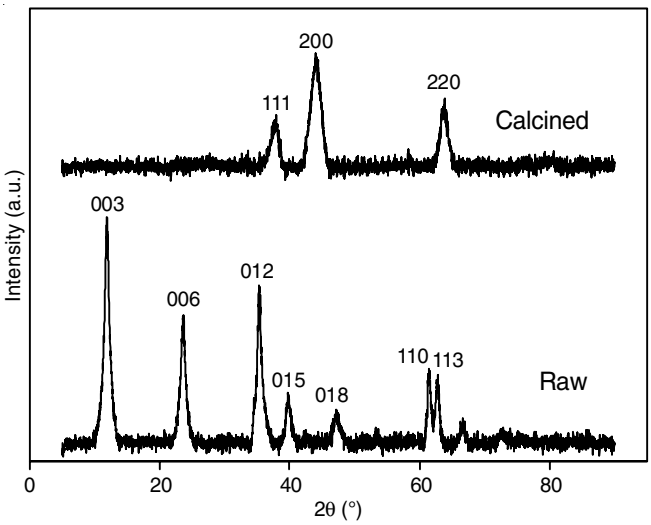

Fig. 2. Powder X-ray diffraction spectra of Ni/Al LDHs

TABLE-2
LATTICE PARAMETERS OF Ni/Al LDHs

Materials	d spacing (Å)	Lattice parameter (Å)	
		a	c
Raw Ni/Al LDH	1.04965	7.44	3.72
Calcined Ni/Al LDH	1.05015	4.02	4.89

After the calcining process, it was found that disappearance of the main basal reflections of (003) and (006) LDH characteristics diffraction peaks shifted to a higher diffraction angle, implying the removal of carbonate and hydroxyl from the interlayer of Ni/Al LDH during calcination process. Three major diffraction peaks were appeared at 37.1º, 43.4º and 63.2º, which can be indexed to (111), (200) and (220) typical peaks for NiO, respectively (JCPDS No. 01-1239). However, the calcined Ni/Al LDH sample does not show the characteristic peaks of alumina oxide due to the poor crystallinity. The PXRD patterns of the calcined samples revealed that there was a total collapse of the hydrotalcite structure after the calcined treatment occurring the formation of Ni and Ni/Al oxides [9]. It has been reported that the calcination process of the Ni/Al LDH precursors leads to the complete disappearance of the PXRD patterns of LDH structure and to the appearance of the characteristic patterns of mixed oxides of NiO-type [10].

Brunauer-Emmett-Teller analysis (BET): The raw and calcined Ni/Al LDH have subjected to N_2 adsorption and desorption analysis in order to investigate their textural properties. The N_2 adsorption and desorption isotherms of the samples raw and calcined Ni/Al LDH are illustrated in Fig. 3. As observed, the graph can be divided into three distinct areas, each area represents a mode of fixation. In the first part, ($0.00 < P/P_o \leq 0.3$), the volume adsorbed increase at low relative pressure area, which implies that this part consists of the adsorption on the monolayer and filling of the micropores. The second part indicates the adsorption through capillary condensation. Finally, the third part corresponds to the filling of meso- and macropores and adsorption on the multilayer. Both materials showed a similar type IV isotherm pattern but with slightly different hysteresis patterns according to the IUPAC classification, suggesting that the materials have mesoporous properties. There are some differences in the behaviour of hysteresis loops, the calcined Ni/Al LDH has the narrowest hysteresis loop compared to the raw Ni/Al LDH. This indicates improved mesoporosity, which is positive feature for catalysis as the diffusional limitations are restricted [9].

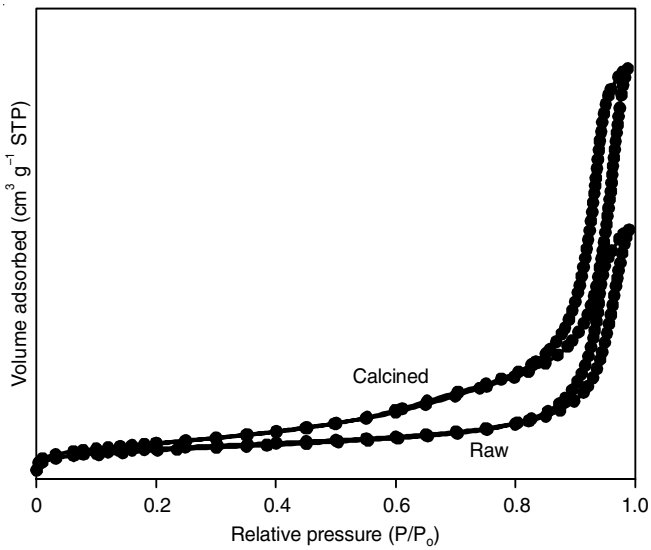

Fig. 3. N_2 adsorption-desorption isotherms of Ni/Al LDHs

The textural properties for the specific surface areas and pore size are summarized in Table-3. The obtained values agree with those already reported for these kinds of materials. The average pore sizes decrease from 24 nm of raw Ni/Al LDH to 19 nm of calcined Ni/Al LDH further proves the formation of pores with a lower size. Moreover, the specific surface area of the calcined Ni/Al LDH increases more than two times when compared with raw Ni/Al LDH from 282 m^2/g to 330 m^2/g. These increases might also indicate that the formation of highly stable spinels avoided, which typically occurs for LDHs containing transition metals cations in the layer and carbonate as counter anion. The high surface area as compared to other LDHs suggests that the synthesized calcined Ni/Al LDH would be suitable candidate for adsorption.

Morphological studies: The FESEM images of raw and calcined Ni/Al LDH are shown in Fig. 4a-f. From the FESEM

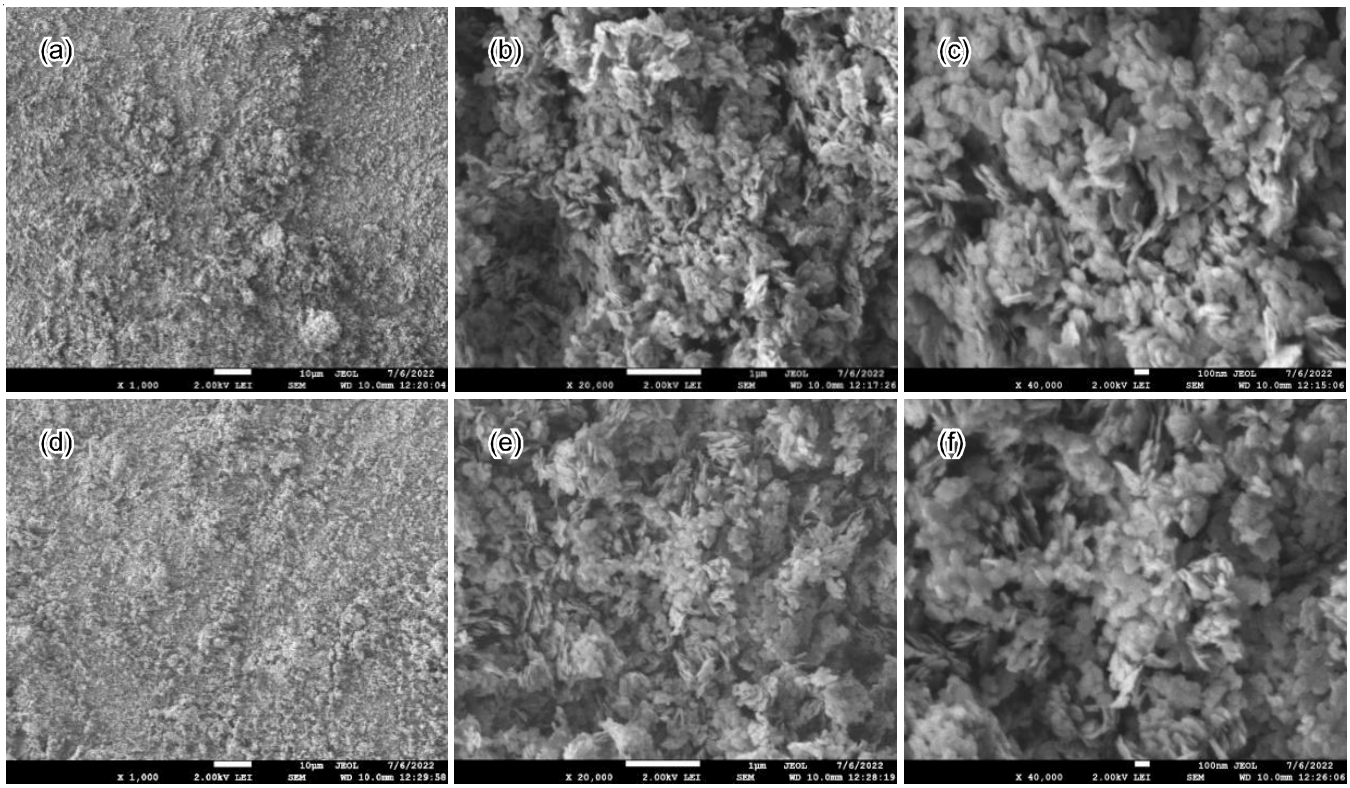

Fig. 4. FESEM images of raw Ni/Al LDH (a,b,c) and calcined Ni/Al LDH (d,e,f)

TABLE-3
TEXTURAL PROPERTIES OF Ni/Al LDHs

Properties	Raw Ni/Al LDH	Calcined Ni/Al LDH
BET surface area (m^2/g)	282	330
BJH adsorption (nm)	24	19
BJH desorption (nm)	18	17
Total volume in pores (cm^2/g)	0.91	1.55

images, it can be seen that all sample display similar morphological features. There is no obvious changes of the samples after calcination. A rough plate-like surface morphology are shown in Fig. 4a and 4d with 5k magnification of raw and calcined Ni/Al LDH. Moreover, as shown in Fig. 4b-c, specially sand roses petal plates with irregular shape of raw Ni/Al LDH could be observed, in good agreement with the above FESEM results. Its unique petal-like nanosheet was also reported earlier [8,11,12]. The structure of raw Ni/Al LDH rough surface with particles of different shapes remained after calcination, as displayed in Fig. 4e-f. The sand roses shape diminished yet still posses its irregular shape.

FTIR studies: FTIR spectroscopy is another useful tool for the characterization of LDHs, involving the vibrations in the octahedral lattice, hydroxyl groups and interlayer anions. A broad absorption band 3446.2 cm^{-1} in the FTIR spectrum of Ni/Al LDH in Fig. 5 can be assigned to the stretching vibration of the hydroxyl groups ($^{-}$OH) of LDH layers and intercalated or adsorbed of water molecules, while in the region spectra band at 1637 cm^{-1} are associated of H–O–H bending vibration with angular deformation of water molecules [13,14]. The main band region of 1340 cm^{-1} is attributed to carbonate/

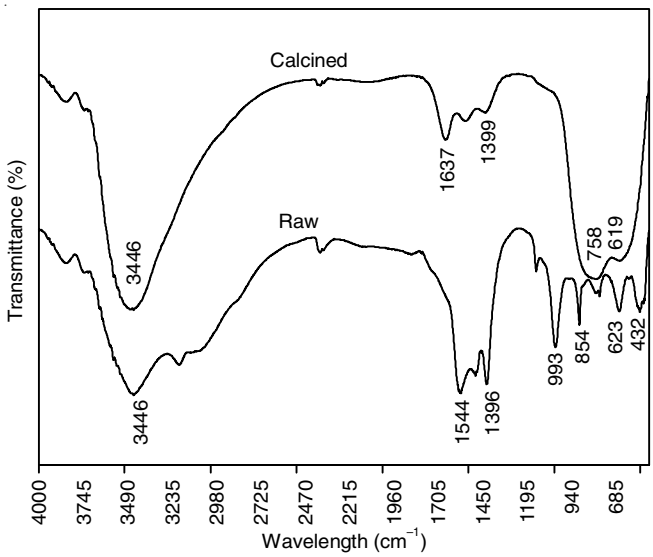

Fig. 5. Infrared spectra of raw and calcined Ni/Al LDHs

nitrate anions and the bands in the region of 650 cm^{-1} are attributed to the M–OH bond, being characteristics of LDH [1,15]. In the spectra, the peaks appeared at 1396.4 cm^{-1} are related to the interlayer CO_3^{2-} group and at 400-800 cm^{-1} are related to the lattice vibration modes of M–O, O–M–O and M–O–M. Therefore, the band at 623 cm^{-1} is related to the spectra of M–O metal oxide stretching vibration in LDH sheets. This difference of the position of the bands can be due to the different metal constituents of the LDH. The details of the infrared wavenumbers and vibrational modes of raw Ni/Al LDH and CNi/Al LDH are shown in Table-4.

TABLE-4
DETAILS OF THE KEY INFRARED WAVENUMBERS AND VIBRATIONAL MODES OF Ni/Al LDHs

Materials	Characteristics band	Wavenumber (cm^{-1}) (This study)	Wavenumber (cm^{-1}) (Ref.)	Ref.
Raw Ni/Al LDH	O–H stretching	3446	3200-3600	[16]
	H–OH bending	1544	1630	[17]
	Interlayer CO_3^{2-}	1396	1300-1600	[18]
	Ni–O, Ni–Al–O stretching	993, 854	400–800	[15]
	Ni–O stretching	623, 432	400-800	[18]
Calcined Ni/Al LDH	O–H stretching	3446	3200-3600	[16]
	H–OH bending	1637	1630	[17]
	N–O stretching	1399	1380	[1]
	Ni–O, Ni–Al–O stretching	758, 619	400-800	[18]

Conclusion

This study examines the synthesis of Ni/Al LDH utilizing an alkali-free co-precipitation technique and evaluates its shape and structure by many techniques including TGA, XRD, BET, FTIR and FESEM. The discussion focuses on the raw and calcined Ni/Al LDH, which demonstrates the structural collapse of hydrotalcite after calcination. The BET analysis reveals the presence of larger surface areas and pore diameters in calcined Ni/Al LDH.

ACKNOWLEDGEMENTS

The support from Universiti Teknologi MARA, UiTM, is gratefully acknowledged.

CONFLICT OF INTEREST

The authors declare that there is no conflict of interests regarding the publication of this article.

REFERENCES

1. W. Bao, H. Tian, Y. Jiang, K. Zhu, R. Zhang, Y. Tan, W. Li, Z. Yu and L. Wang, *Ionics*, **25**, 3859 (2019); https://doi.org/10.1007/s11581-019-02952-3
2. L. Fan, L. Yang, Y. Lin, G. Fan and F. Li, *Polym. Degrad. Stab.*, **176**, 109153 (2020); https://doi.org/10.1016/j.polymdegradstab.2020.109153
3. R. Benhiti, A. Ait Ichou, A. Zaghloul, R. Aziam, G. Carja, M. Zerbet, F. Sinan and M. Chiban, *Environ. Sci. Pollut. Res. Int.*, **27**, 45767 (2020); https://doi.org/10.1007/s11356-020-10444-5
4. Z. Lv, S. Yang, H. Zhu, L. Chen, N.S. Alharbi, M. Wakeel, A. Wahid and C. Chen, *Appl. Surf. Sci.*, **448**, 599 (2018); https://doi.org/10.1016/j.apsusc.2018.04.162
5. N.A. Tajuddin, J.C. Manayil, A.F. Lee and K. Wilson, *Catalysts*, **12**, 286 (2022); https://doi.org/10.3390/catal12030286
6. S. Pa, H.M. Afzal and M.A. Al-Harthi, *Polym. Compos.*, **41**, 4253 (2020); https://doi.org/10.1002/pc.25708
7. N.R. Palapa, R. Mohadi and A. Lesbani, *AIP Conf. Proc.*, **2026**, 020018 (2018); https://doi.org/10.1063/1.5064978
8. N.R. Palapa, T. Taher, R. Mohadi, A. Rachmat, M. Mardiyanto, M. Miksusanti and A. Lesbani, *Chem. Eng. Commun.*, **209**, 684 (2021); https://doi.org/10.1080/00986445.2021.1895773
9. N. Taoufik, W. Boumya, A. Elhalil, M. Achak, M. Sadiq, M. Abdennouri and N. Barka, *Int. J. Environ. Anal. Chem.*, **103**, 712 (2021); https://doi.org/10.1080/03067319.2020.1863387
10. Y.R. Dias and O.W. Perez-Lopez, *J. CO2 Util.*, **68**, 102381 (2023); https://doi.org/10.1016/j.jcou.2022.102381
11. S. Shen, W. Guo, W. Zhuang, W.J. Yang, L. Qin, X. Liu and Z. Yue, *J. Phys. Conf. Ser.*, **2009**, 012008 (2021); https://doi.org/10.1088/1742-6596/2009/1/012008
12. X. Hu, P. Li, X. Zhang, B. Yu, C. Lv, N. Zeng, J. Luo, Z. Zhang, J. Song and Y. Liu, *Nanomaterials*, **9**, 1688 (2019); https://doi.org/10.3390/nano9121688
13. S. Jaerger and F. Wypych, *J. Appl. Polym. Sci.*, **48737**, 1 (2019); https://doi.org/10.1002/app.48737
14. W.M.A. El Rouby, S.I. El-Dek, M.E. Goher and S.G. Noaemy, *Environ. Sci. Pollut. Res. Int.*, **27**, 18985 (2020); https://doi.org/10.1007/s11356-018-3257-7
15. E.N. Alkhafaji, *IOP Conf. Ser. Mater. Sci. Eng.*, **871**, 012021 (2020); https://doi.org/10.1088/1757-899X/871/1/012021
16. A. Machrouhi, M. Khnifira, W. Boumya, M. Sadiq, M. Abdennouri, A. Elhalil, F.Z. Mahjoubi and N. Barka, *Chem. Phys. Impact*, **6**, 100214 (2023); https://doi.org/10.1016/j.chphi.2023.100214
17. A. Hanif, M. Sun, S. Shang, Y. Tian, A.C.K. Yip, Y.S. Ok, I.K.M. Yu, D.C.W. Tsang, Q. Gu and J. Shang, *J. Hazard. Mater.*, **374**, 365 (2019); https://doi.org/10.1016/j.jhazmat.2019.04.049
18. S. Charafi, F.Z. Janani, A. Elhalil, M. Abdennouri, M. Sadiq and N. Barka, *Biointerface Res. Appl. Chem.*, **13**, 265 (2022); https://doi.org/10.33263/BRIAC133.265